Ruling Out Possible Secondary Stars to Exoplanet Host Stars Using the CHARA Array

Ellyn K. Baines[†]

Remote Sensing Division, Naval Research Laboratory, 4555 Overlook Avenue SW, Washington, DC 20375

ellyn.baines.ctr@nrl.navy.mil

Harold A. McAlister, Theo A. ten Brummelaar, Nils H. Turner, Judit Sturmann, Laszlo Sturmann, P. J. Goldfinger, Christopher D. Farrington

Center for High Angular Resolution Astronomy, Georgia State University, P.O. Box 3969, Atlanta, GA 30302-3969

hal@chara.gsu.edu, theo@chara-array.org, nils@chara-array.org, judit@chara-array.org, sturmann@chara-array.org, pj@chara-array.org, farrington@chara-array.org

Stephen T. Ridgway

Kitt Peak National Observatory, National Optical Astronomy Observatory, P.O. Box 26732, Tucson, AZ 85726-6732

ridgway@noao.edu

ABSTRACT

Of the over 450 exoplanets known to date, more than 420 of them have been discovered using radial velocity studies, a method that tells nothing about the inclination of the planet's orbit. Because it is more likely that the companion is a planetary-mass object in a moderate- to high-inclination orbit than a low-mass stellar object in a nearly face-on orbit, the secondary bodies are presumed to be planets. Interferometric observations allow us to inspect the angular diameter

[†]The observations described here were completed while with the Center for High Angular Resolution Astronomy, Georgia State University, P.O. Box 3969, Atlanta, GA 30302-3969.

For preprints, please email ellyn.baines.ctr@nrl.navy.mil.

Report Documentation Page

Form Approved
OMB No. 0704-0188

1. REPORT DATE	2. REPORT TYPE	3. DATES COVERED
17 MAY 2010		**00-00-2010 to 00-00-2010**

4. TITLE AND SUBTITLE	5a. CONTRACT NUMBER
Ruling Out Possible Secondary Stars to Exoplanet Host Stars Using the CHARA Array	5b. GRANT NUMBER
	5c. PROGRAM ELEMENT NUMBER
6. AUTHOR(S)	5d. PROJECT NUMBER
	5e. TASK NUMBER
	5f. WORK UNIT NUMBER
7. PERFORMING ORGANIZATION NAME(S) AND ADDRESS(ES) **Remote Sensing Division,Naval Research Laboratory,4555 Overlook Avenue SW,Washington,DC,20375**	8. PERFORMING ORGANIZATION REPORT NUMBER
9. SPONSORING/MONITORING AGENCY NAME(S) AND ADDRESS(ES)	10. SPONSOR/MONITOR'S ACRONYM(S)
	11. SPONSOR/MONITOR'S REPORT NUMBER(S)

12. DISTRIBUTION/AVAILABILITY STATEMENT
Approved for public release; distribution unlimited

13. SUPPLEMENTARY NOTES

14. ABSTRACT

Of the over 450 exoplanets known to date, more than 420 of them have been discovered using radial velocity studies, a method that tells nothing about the inclination of the planet's orbit. Because it is more likely that the companion is a planetary-mass object in a moderate- to high-inclination orbit than a low-mass stellar object in a nearly face-on orbit, the secondary bodies are presumed to be planets. Interferometric observations allow us to inspect the angular diameter fit residuals to calibrated visibilities in order to rule out the possibility of a lowmass stellar companion in a very low-inclination orbit. We used the Center for High Angular Resolution Astronomy (CHARA) Array interferometer to observe 20 exoplanet host stars and considered five potential secondary spectral types G5 V, K0 V, K5 V, M0 V, and M5 V. If a secondary star is present and is sufficiently bright, the effects of the added light will appear in interferometric observations where the planet will not. All secondary types could be eliminated from consideration for 7 host stars and no secondary stars of any spectral type could be ruled out for 7 more. The remaining 6 host stars showed a range of possible secondary types.

15. SUBJECT TERMS

16. SECURITY CLASSIFICATION OF:			17. LIMITATION OF ABSTRACT	18. NUMBER OF PAGES	19a. NAME OF RESPONSIBLE PERSON
a. REPORT	b. ABSTRACT	c. THIS PAGE			
unclassified	**unclassified**	**unclassified**	**Same as Report (SAR)**	**7**	

fit residuals to calibrated visibilities in order to rule out the possibility of a low-mass stellar companion in a very low-inclination orbit. We used the Center for High Angular Resolution Astronomy (CHARA) Array interferometer to observe 20 exoplanet host stars and considered five potential secondary spectral types: G5 V, K0 V, K5 V, M0 V, and M5 V. If a secondary star is present and is sufficiently bright, the effects of the added light will appear in interferometric observations where the planet will not. All secondary types could be eliminated from consideration for 7 host stars and no secondary stars of any spectral type could be ruled out for 7 more. The remaining 6 host stars showed a range of possible secondary types.

Subject headings: binaries: general — infrared: stars — planetary systems — techniques: interferometric

1. Introduction

Radial velocity observations of exoplanet systems alone are insufficient to distinguish between intermediate- to high-inclination planetary systems and low-inclination binary star systems. Stepinski & Black (2001) estimated probability densities of orbital periods and eccentricities for two samples: exoplanet candidates and spectroscopic binary star systems with solar-type primary stars. They found the distributions of the two populations were statistically indistinguishable in the context of orbital elements.

In an earlier study, Imbert & Prévot (1998) modeled nine exoplanet systems as binary star systems to test if the radial velocity observations could be reproduced by low-mass stellar companions. Although the probability of binary star systems appearing as planetary systems was low – 0.01 to 4% – the model results described the observations satisfactorily and showed it is possible for a binary star system to mimic an exoplanet system.

While it is unlikely that there are unseen stellar companions with very low inclinations masquerading as exoplanets, the only way to exclude the possibility of a low-inclination star observationally is to study the system at angular scales comparable to the calculated star-planet separation. These separations are on the order of 0.5 to 5.0 milliarcseconds, and the only relevant technique applicable is interferometry, which we present here for 20 exoplanet host stars.

The probability of a system's inclination being in the range i to $i + \Delta i$ is proportional to the ratio of the surface element of a hemisphere defined by that range and integrated over the azimuth angle (Φ) to the surface area of the entire hemisphere. The area element for a

given range of i is:

$$\mathrm{d}A = \mathrm{d}i \times \sin i \, \mathrm{d}\Phi, \tag{1}$$

and the probability of a system having a specific range of i is:

$$P_{i,i+\Delta i} = \frac{\int_0^{2\pi} \int_i^{i+\Delta i} \sin i \, \mathrm{d}i \, \mathrm{d}\Phi}{\int_0^{2\pi} \int_0^{\pi/2} \sin i \, \mathrm{d}i \, \mathrm{d}\Phi} = \frac{-2\pi \, \cos i \, |_i^{i+\Delta i}}{-2\pi \, \cos i \, |_0^{\pi/2}} = \cos i - \cos(i + \Delta i). \tag{2}$$

Therefore the probability of an orbit with an inclination below 45° is ∼30% while the probability of the orbit having an inclination higher than 45° is ∼70%. The inclinations necessary for the companion to be stellar in nature are very low, on the order of less than one degree. This means the probability of any given system being a binary star is correspondingly low ($\sim 10^{-4}$%) and it would take much larger sample size than is available to have a good chance of finding a stellar companion masquerading as a planet. When taken as a whole, the chances of finding a stellar companion in this sample are only on the order of 10^{-5}.

We are not trying to prove that the apparent companion for any given system is a low-mass star instead of a planet, but instead are using our observations to rule out certain types of stellar companions for each star observed. Radial velocity studies alone cannot perform this task, and interferometry is well suited to further our knowledge of exoplanet host stars. When we are able to be more confident that they are indeed planetary systems and not face-on binary stars, we further characterize the host stars themselves as well as contribute to the statistics that tell us what percentage of stars host planets versus how many have stellar companions.

An important criteria for the detection or non-detection of otherwise unseen secondary stars is the magnitude difference between the known primary and the putative secondary stars. Simulations using a program written by Theo ten Brummelaar that realistically models instrumental and atmospheric noises, as well as observations of pairs of known brightness contrasts, indicate that the Array is sensitive to a magnitude difference in the K-band (ΔK) of 3.0. Therefore, if a second star is present and is not more than ∼3.0 magnitudes fainter than the host star, the effects of the second star will be seen in the interferometric data. It should be noted that a limiting magnitude difference in the K-band (ΔK) of 3.0 is a lower limit, as the true ΔK also depends on the absolute brightness of the two stars and could be slightly higher for some systems.

This technique of using interferometric observations to eliminate the possibility of certain types of secondary stars was employed to examine the exoplanet host star 51 Peg (HD 217014) by Boden et al. (1998), whose analysis of Palomar Testbed Interferometer data supported a single-star model for that star. They fit single-star and binary-star models to the data and

found that any possible unseen stellar companion would have to have a K magnitude fainter than 7.30 and a mass of less than $0.22M_{\odot}$.

Here we describe our interferometric observations, our method for choosing calibrator stars, and define the role interferometric resolution plays in Section 2. In Section 3, we discuss how the angular diameter fit residuals to calibrated visibilities can help us eliminate certain types of secondary stars, and Section 4 explores the implications of the observations. This paper is follow-on work to an earlier study (Baines et al. 2008b).

2. Interferometric Observations

All observations were obtained using the CHARA Array, a six-element optical/infrared interferometric array located on Mount Wilson, California (ten Brummelaar et al. 2005). We used the pupil-plane "CHARA Classic" beam combiner in the K'-band (2.133 μm center with a 0.349 μm width) while visible wavelengths (470-800 nm) were used for tracking and tip/tilt corrections. The observing procedure and data reduction process employed here are described in McAlister et al. (2005). The observable quantity from an interferometer is the fringe contrast or "visibility" of the observed target, and each dataset consists of approximately 200 scans across the fringe.

Our target list was selected from the complete exoplanet list by using declination limits and magnitude constraints: north of -10° declination, brighter than $V = +10$ in order for the tip/tilt system to lock onto the star, and brighter than $K = +6.5$ for reliable fringe detection with a sufficiently high signal-to-noise ratio. We obtained data on the 20 exoplanet host stars between October 2005 and September 2008. The observations were taken using mostly the longest baseline available on the CHARA Array (331 m), though 156-m and 249-m baselines were also used.

Reliable calibrators stars are critical in interferometric observations, acting as the standard against which the science target is measured, and the ideal calibrator is a single, spherical, non-variable star. Our observing pattern was calibrator-target-calibrator so that every target was bracketed by calibrator observations made as close in time as possible; therefore "5 bracketed observations" denotes 5 target and 6 calibrator data sets. The target-calibrator (T-C) distances ranged from 1 to 9° and 13 calibrators were within 4° of their target stars. This allowed us to observe the stars as close together in time as possible, usually on the order of 3 to 5 minutes between the two, therefore reducing the effects of changing seeing conditions as much as possible. Table 1 lists the exoplanet host stars observed, their calibrators, the dates of the observations, the baseline used, the number of observations obtained,

and the T-C distance.

In order to check for excess emission that could indicate a low-mass stellar companion or circumstellar disk, we fitted spectral energy distributions (SEDs) based on published $UBVRIJHK$ photometric values for each calibrator star. Limb-darkened diameters were calculated using Kurucz model atmospheres[1] based on effective temperature and gravity values obtained from the literature. The models were then fit to observed photometric values also from the literature after converting magnitudes to fluxes using Colina et al. (1996) for $UBVRI$ values and Cohen et al. (2003) for JHK values.

Many of the calibrator stars chosen here had been used as comparison or calibrator stars in other studies, or speckle studies did not find companions (see Table 2). For those calibrator stars that had not been previously observed, their SED fits showed no excess flux that could indicate a stellar companion that would then contaminate our interferometric observations.

Our ability to detect stellar companions depends on two main factors. The first is the precision of our visibility measurements. The higher the precision, the higher our sensitivity to finding a secondary companion. The second factor is whether the measured angular diameters or potential primary-secondary separation would be resolved in our data. The resolution of an interferometer depends on the wavelength used and the distance between the telescopes, otherwise known as the baseline. A star is considered unresolved if its visibility is $\cong$1 and is completely resolved when its visibilities drop to zero. Different sized stars will be resolved at different baselines (see Figure 1).

Another effect to account for is bandwidth smearing, which occurs when the physical width of the filter's bandpass affects the measurements as the resolution varies across the band. Bandwidth smearing is only significant when a star's angular diameter exceeds the coherent field of view of the interferometer, which is calculated to be

$$\mathrm{FOV} = \frac{\theta_{\mathrm{min}}}{\pi} \left(\frac{\Delta\lambda}{\lambda_0} \right)^{-1}, \tag{3}$$

where $\theta_{\mathrm{min}} = \lambda_0/B$ and B is the baseline, λ_0 is the central wavelength of the filter, and $\Delta\lambda$ is the width of the filter (Tango & Davis 2002). Because our coherent FOV is larger than the measured angular diameters in all cases, we do not need to correct for this effect when measuring our primary exoplanet host stars. On the other hand, when we determine the visibilities for binary systems that have calculated separations larger than the FOV, we need

[1]See http://kurucz.cfa.harvard.edu.

to account for bandwidth smearing by using a modified version of the visibility equation for binary stars.

3. Characterizing Angular Diameter Fit Residuals to Calibrated Visibilities

To determine stellar angular diameters, measured visibilities (V) are fit to a model of a uniformly-illuminated disk (UD). Single-star diameter fits to V were based upon the UD approximation given by $V = [2J_1(x)]/x$, where J_1 is the first-order Bessel function and $x = \pi B \theta_{\rm UD} \lambda^{-1}$, where B is the projected baseline at the star's position, $\theta_{\rm UD}$ is the apparent UD angular diameter of the star, and λ is the effective wavelength of the observation (Shao & Colavita 1992). A more realistic model of a star's disk involves limb-darkening (LD), and the relationship incorporating the linear limb darkening coefficient μ_λ (Hanbury-Brown et al. 1974) is:

$$V = \left(\frac{1-\mu_\lambda}{2} + \frac{\mu_\lambda}{3}\right)^{-1} \times \left[(1-\mu_\lambda)\frac{J_1(\mathrm{x})}{\mathrm{x}} + \mu_\lambda \left(\frac{\pi}{2}\right)^{1/2} \frac{J_{3/2}(\mathrm{x})}{\mathrm{x}^{3/2}}\right]. \quad (4)$$

Table 3 lists the Modified Julian Date (MJD), baseline B, projected baseline position angle (Θ), calibrated visibility (V_c), and error in V_c (σV_c) for each star observed, and the resulting angular diameters are presented in Table 4. Figure 2 shows the LD diameter fit for HD 164922 as this star's diameter is presented for the first time here. Similar plots for the remaining stars can be found in the references listed in Table 4.

The systematics in the residuals of the angular diameter fit to measured visibilities can help us eliminate certain types of potential secondary stars. The smaller the residuals, the lower the chance of an unseen stellar companion. For each exoplanet host star observed, a variety of secondary stars were considered: G5 V, K0 V, K5 V, M0 V, and M5 V. The magnitude difference ($\Delta \mathrm{M}_K$, listed as ΔK in the tables) and angular separation (α) of a face-on orbit between the host star and companion were calculated for each possible pairing:

$$\Delta \mathrm{M}_K = \mathrm{M_s} + (\mathrm{m_h} - \mathrm{M_h}) - \mathrm{m_h}, \quad (5)$$

where $\mathrm{M_{h,s}}$ are the absolute magnitudes of the host star and potential secondary, respectively, $\mathrm{m_h}$ is the apparent magnitude of the host star, and

$$(\mathrm{m_h} - \mathrm{M_h}) = 5 \log\left(\frac{100}{\pi}\right), \quad (6)$$

where π is the host star's parallax in milliarcseconds (mas). An estimate of the angular separation α in mas was calculated from Kepler's Third Law:

$$\alpha = \left[(M_\mathrm{h} + M_\mathrm{s}) \times P^2\right]^{\frac{1}{3}} \times \pi, \quad (7)$$

where $M_{\rm h,s}$ are the masses in $M_\odot$ of the exoplanet's host star and potential secondary star, respectively, and P is the companion's orbital period in years.

The angular diameter (θ) for each possible secondary star was estimated using the calibration of radius as a function of spectral type from Cox (2000) and the parallax of the host star. The masses and radii in Cox are based on values derived from Habets & Heintze (1981), who observed binary stars in order to create empirical relationships between various stellar parameters as a function of luminosity class. Tables 4 and 5 present the results of these calculations.

The resulting values for θ, ΔK, and α were then used to determine the visibility curve for a single star with the host star's measured angular diameter as well as for a binary system with the parameters listed above. The equation used to calculate the visibility curve for a binary system when observed using a narrow bandpass is

$$V = (1+\beta)^{-1}[V_1^2 + \beta^2 V_2^2 + 2\beta V_1 V_2 \cos\{2\pi B\lambda^{-1}\alpha\cos\phi\}]^{\frac{1}{2}}, \tag{8}$$

where $V_{1,2}$ are the visibilities for the primary and secondary star, respectively, $\beta = 100^{0.2\Delta \rm m}$ where Δm is the magnitude difference between the two stars, and ϕ is the difference of the position angles between the binary and baseline (Hanbury-Brown et al. 1970). Because the observations described here were taken using a filter with a bandpass of $\sim 16\%$, the equation needs to be modified to include the effects of wide bandwidth and bandwidth smearing (North et al. 2007):

$$V = (1+\beta)^{-1}[\beta^2 V_1^2 + V_2^2 + 2\beta r(\psi) V_1 V_2 \cos\psi]^{\frac{1}{2}}, \tag{9}$$

where $\psi = 2\pi B\lambda^{-1}\alpha\cos\phi$ and

$$r(\psi) = \exp\left(\frac{-\Delta\lambda^2}{\lambda_0^2}\frac{\psi^2}{32\ln 2}\right). \tag{10}$$

To explore the effects of the projected position angle of a binary star vector separation, we calculated the residuals using position angles of 0°, 30°, and 60° (see Table 6).

To estimate the detection sensitivity, the largest difference between the visibility curves for a single star and for a binary system with the parameters listed in Table 5 was calculated. This quantity, $\Delta V_{\rm max}$, then represented the maximum deviation of the binary visibility curve from the single-star curve. Figure 3 shows an example of this.

Due to uncertainties in such input parameters as the host star's mass, parallax, and the planet's orbital period used in Equations 3 and 4, we did not believe a 1σ threshold would be a reliable diagnostic. Therefore, in order to rule out putative stellar companions,

we selected a lower limit of $2\sigma_{\rm res}$, where $\sigma_{\rm res}$ is the standard deviation of the residuals to the diameter fit; i.e., if $\Delta V_{\rm max} \geq 2\sigma_{\rm res}$ for a given secondary component, that particular spectral type can be eliminated as a possible stellar companion. If $\Delta V_{\rm max} < 2\sigma_{\rm res}$, the effects of the companion would not be clearly seen in the visibility curve, and that spectral type cannot be ruled out. For each exoplanet host star, Table 6 lists the observed $\sigma_{\rm res}$ and the predicted $\Delta V_{\rm max}$ for each secondary type considered.

4. Results and Discussion

Though the errors for the individual calibrated visibilities listed in Table 3 are on the order of 2-20%, the errors for the angular diameter fits to these visibilities are on the order of 1-6% for most stars. This is because the calibrated visibility errors are overestimated. This can be best illustrated by performing the diameter fit to the data. For each $\theta_{\rm LD}$ fit, the errors were derived via the reduced χ^2 minimization method (Wall & Jenkins 2003; Press et al. 1992): the diameter fit with the lowest χ^2 was found and the corresponding diameter was the final $\theta_{\rm LD}$ for the star. The errors were calculated by finding the diameter at $\chi^2 + 1$ on either side of the minimum χ^2 and determining the difference between the χ^2 diameter and $\chi^2 + 1$ diameter. In calculating the diameter errors in Table 4, we adjusted the estimated visibility errors to force the reduced χ^2 to unity because when this is omitted, the reduced χ^2 is well under 1.0, indicating we are overestimating the errors in our calibrated visibilities.

In addition to measuring the angular diameters of these stars interferometrically, we also estimated their diameters using two methods to check for discrepancies. We performed SED fits using the method described in Section 2 as well as using the relationship described in Kervella et al. (2004) between the $(V - K)$ color and log $\theta_{\rm LD}$. Table 8 lists the results of these calculations and Figure 4 plots $\theta_{\rm SED}$ and $\theta_{(V-K)}$ versus $\theta_{\rm measured}$. For stars larger than ∼0.7 mas, the errors in the estimated diameters are larger than those for the measured diameters.

In order to characterize the scatter in the diameters of the entire sample, the standard deviation σ of the quantity $|\theta_{\rm LD} - \theta_{\rm SED}|$ was determined to be 8%, which indicates a fairly good correspondence between the estimated and measured diameters. For comparison purposes, the standard deviation of $|\theta_{(V-K)} - \theta_{\rm SED}|$ was 12%. Four of the 20 stars in the sample have measured diameters that are not within 1-sigma of the diameters estimated using either SED fits or $(V - K)$ color. Three of the four (HD 145675, HD 154345, and HD 185269) are among the smallest stars measured and have some of the highest diameter errors in the sample, ranging from 6% to 11%.

The largest outlier is HD 217107, which we measured at 0.70±0.01 mas while the diameters from SED fits and $(V-K)$ color were 0.52±0.02 mas and 0.54±0.02 mas, respectively. There are no signs of variability indicated in the literature for the star that would impact the diameters estimated using photometry. While the calibrator was small (0.31±0.01 mas), showed no signs of having a stellar companion using speckle (McAlister et al. 1987) or in the SED fit, and was used as a photometric comparison star for HD 217107 (Vogt et al. 2005), it could be the cause of the discrepancy in the angular diameter estimates and interferometric measurements. Future observations of HD 217107 using the CHARA Array and different calibrators should help clarify the situation.

The star that showed the most potential for being a binary system instead of a planetary system was the newly-presented HD 164922. The visibility points show a slight sinusoidal pattern, though there are not enough observations to reliably fit the data to a binary star model. Future planned observations using the CHARA Array over a longer time should provide more details on the star.

No secondary spectral types could be eliminated from consideration for 7 exoplanet hosts, while all spectral types could be discounted for 7 host stars. The remaining 6 host stars had some but not all of the various secondary types ruled out. Because of the small sample size, we did not expect to find any stellar companions masquerading as planets, as the probability of a moderate- to high-inclination planet mimicking a face-on stellar companion is very low. Our contribution was eliminate the possibility of certain secondary spectral types for the host stars.

The CHARA Array is funded by the National Science Foundation through NSF grant AST-0908253 and by Georgia State University through the College of Arts and Sciences, and STR acknowledges partial support by NASA grant NNH09AK731. This research has made use of the SIMBAD literature database, operated at CDS, Strasbourg, France, and of NASA's Astrophysics Data System. This publication makes use of data products from the Two Micron All Sky Survey, which is a joint project of the University of Massachusetts and the Infrared Processing and Analysis Center/California Institute of Technology, funded by the National Aeronautics and Space Administration and the National Science Foundation.

REFERENCES

Allende Prieto, C., & Lambert, D. L. 1999, A&A, 352, 555

Baines, E. K., McAlister, H. A., ten Brummelaar, T. A., Turner, N. H., Sturmann, J., Sturmann, L., Goldfinger, P. J., & Ridgway, S. T. 2008a, ApJ, 680, 728

Baines, E. K., McAlister, H. A., Brummelaar, T. A. t., Turner, N. H., Sturmann, J., Sturmann, L., & Ridgway, S. T. 2008b, ApJ, 682, 577

Baines, E. K., McAlister, H. A., Ten Brummelaar, T. A., Sturmann, J., Sturmann, L., Turner, N. H., & Ridgway, S. T. 2009, ApJ, 701, 154

Baines, E. K., et al. 2010, ApJ, 710, 1365

Bartkevicius, A., & Gudas, A. 2001, Baltic Astronomy, 10, 481

Berger, D. H., et al. 2006, ApJ, 644, 475

Boden, A. F., et al. 1998, ApJ, 504, L39

Butler, R. P., Marcy, G. W., Vogt, S. S., Fischer, D. A., Henry, G. W., Laughlin, G., & Wright, J. T. 2003, ApJ, 582, 455

Butler, R. P., et al. 2006, ApJ, 646, 505

Cayrel de Strobel, G., Soubiran, C., Friel, E. D., Ralite, N., & Francois, P. 1997, A&AS, 124, 299

Cohen, M., Wheaton, W. A., & Megeath, S. T. 2003, AJ, 126, 1090

Colina, L., Bohlin, R. C., & Castelli, F. 1996, AJ, 112, 307

Cox, A. N. 2000, Allen's astrophysical quantities, 4th ed., ed. A. N. Cox (New York: AIP Press; Springer)

Cutri, R. M., et al. 2003, The IRSA 2MASS All-Sky Point Source Catalog, NASA/IPAC Infrared Science Archive

Döllinger, M. P., Hatzes, A. P., Pasquini, L., Guenther, E. W., Hartmann, M., Girardi, L., & Esposito, M. 2007, A&A, 472, 649

Döllinger, M. P., Hatzes, A. P., Pasquini, L., Guenther, E. W., Hartmann, M., & Girardi, L. 2009a, A&A, 499, 935

Döllinger, M. P., Hatzes, A. P., Pasquini, L., Guenther, E. W., & Hartmann, M. 2009b, A&A, 505, 1311

ESA 1997, VizieR Online Data Catalog, 1239, 0

Fischer, D. A., Marcy, G. W., Butler, R. P., Vogt, S. S., & Apps, K. 1999, PASP, 111, 50

Fischer, D. A., Marcy, G. W., Butler, R. P., Vogt, S. S., Walp, B., & Apps, K. 2002, PASP, 114, 529

Habets, G. M. H. J., & Heintze, J. R. W. 1981, A&AS, 46, 193

Hanbury Brown, R., Davis, J., Herbison-Evans, D., & Allen, L. R. 1970, MNRAS, 148, 103

Hanbury-Brown, R., Davis, J., Lake, R. J. W., & Thompson, R. J. 1974, MNRAS, 167, 475

Hatzes, A. P., Cochran, W. D., Endl, M., McArthur, B., Paulson, D. B., Walker, G. A. H., Campbell, B., & Yang, S. 2003, ApJ, 599, 1383

Hatzes, A. P., Guenther, E. W., Endl, M., Cochran, W. D., Döllinger, M. P., & Bedalov, A. 2005, A&A, 437, 743

Imbert, M., & Prévot, L. 1998, A&A, 334, L37

Johnson, J. A., Marcy, G. W., Fischer, D. A., Henry, G. W., Wright, J. T., Isaacson, H., & McCarthy, C. 2006, ApJ, 652, 1724

Johnson, J. A., et al. 2007, ApJ, 665, 785

Kervella, P., Thévenin, F., Di Folco, E., & Ségransan, D. 2004, A&A, 426, 297

Konacki, M., & Lane, B. F. 2004, ApJ, 610, 443

McAlister, H. A., Hartkopf, W. I., Hutter, D. J., Shara, M. M., & Franz, O. G. 1987, AJ, 93, 183

McAlister, H. A., Hartkopf, W. I., Sowell, J. R., Dombrowski, E. G., & Franz, O. G. 1989, AJ, 97, 510

McAlister, H. A., et al. 2005, ApJ, 628, 439

Mermilliod, J. C. 1991, Catalogue of Homogeneous Means in the UBV System, Institut d'Astronomie, Universite de Lausanne

Monet, D. G., et al. 2003, AJ, 125, 984

Neugebauer, G., & Leighton, R. B. 1969, NASA SP, Washington: NASA, 1969

North, J. R., Tuthill, P. G., Tango, W. J., & Davis, J. 2007, MNRAS, 377, 415

Press, W. H., Teukolsky, S. A., Vetterling, W. T., & Flannery, B. P. 1992, Numerical recipes in C. The art of scientific computing (Cambridge: University Press, c1992, 2nd ed.)

Prugniel, P., Soubiran, C., Koleva, M., & Le Borgne, D. 2007, VizieR Online Data Catalog, 3251, 0

Sato, B., et al. 2008a, PASJ, 60, 539

Sato, B., et al. 2008b, PASJ, 60, 1317

Schuler, S. C., Kim, J. H., Tinker, M. C., Jr., King, J. R., Hatzes, A. P., & Guenther, E. W. 2005, ApJ, 632, L131

Shao, M., & Colavita, M. M. 1992, ARA&A, 30, 457

Soubiran, C., Le Campion, J. F., Cayrel de Strobel, G., & Caillo, A. 2010, arXiv:1004.1069

Stepinski, T. F., & Black, D. C. 2001, A&A, 371, 250

Tango, W. J., & Davis, J. 2002, MNRAS, 333, 642

ten Brummelaar, T. A., et al. 2005, ApJ, 628, 453

van Belle, G. T., et al. 2008, ApJS, 176, 276

van Leeuwen, F. 2007, Hipparcos, the New Reduction of the Raw Data (Cambridge, UK Series: Astrophysics and Space Science Library; Springer)

Vogt, S. S., Butler, R. P., Marcy, G. W., Fischer, D. A., Henry, G. W., Laughlin, G., Wright, J. T., & Johnson, J. A. 2005, ApJ, 632, 638

Wall, J. V., & Jenkins, C. R. 2003, Practical Statistics for Astronomers (Princeton Series in Astrophysics)

Wittenmyer, R. A., et al. 2005, ApJ, 632, 1157

Wright, J. T., Marcy, G. W., Butler, R. P., Vogt, S. S., Henry, G. W., Isaacson, H., & Howard, A. W. 2008, ApJ, 683, L63

Table 1. Observing Log.

Target HD	Calibrator HD	Baseline (max. length)	Date (UT)	# Obs	T-C Sep (deg)
10697	10477	S1-E1 (331 m)	2005 Oct 23	4	4
			2007 Sep 14	4	
13189	11007	S1-E1 (331 m)	2005 Dec 12	4	4
			2006 Aug 14	4	
32518	31675	S1-E1 (331 m)	2007 Nov 14	9	3
45410	46590	S1-E1 (331 m)	2008 Sep 11	5	2
50554	49736	S1-E1 (331 m)	2005 Dec 12	5	2
73108	69548	E2-W2 (156 m)	2008 May 9	5	7
136726	145454	E2-W2 (156 m)	2008 May 9	6	6
139357	132254	S1-E1 (331 m)	2007 Sep 14	4	7
145675	151044	S1-E1 (331 m)	2006 Aug 12	6	8
154345	151044	S1-E1 (331 m)	2008 Sep 10	7	4
164922	159139	S1-E1 (331 m)	2008 Aug 11	5	7
167042	161693	S1-E1 (331 m)	2007 Sep 15	8	4
170693	172569	W1-S2 (249 m)	2007 Sep 3	4	1
185269	184381	S1-E1 (331 m)	2008 Jul 18	15	3
			2008 Jul 20	5	
188310	182101	S1-E1 (331 m)	2008 Sep 8	8	8
199665	194012	S1-E1 (331 m)	2008 Sep 8	10	9
210702	210074	S1-E1 (331 m)	2008 Sep 8	4	4
217107	217131	S1-E1 (331 m)	2008 Sep 8	5	1
221345	222451	S1-E1 (331 m)	2008 Sep 11	5	3
222404	219485	S1-E1 (331 m)	2008 Sep 11	7	4

Note. — The three arms of the Array are denoted by their cardinal directions: "S" is south, "E" is east, and "W" is west. Each arm bears two telescopes, numbered "1" for the telescope farthest from the beam combining laboratory and "2" for the telescope closer to the lab.

Table 2. Notes on Calibrator Quality and Previous Uses.

HD	
10477	No sign of duplicity in literature or SED fit
11007	Listed as a "suitable" calibrator in van Belle et al. (2008); used as calibrator in Konacki & Lane (2004)
31675	No companion found using speckle in McAlister et al. (1989)
46590	No sign of duplicity in literature or SED fit
49736	No sign of duplicity in literature or SED fit
69548	No sign of duplicity in literature or SED fit
132254	Listed as a "probably suitable" calibrator in van Belle et al. (2008); no companion found using speckle in McAlister et al. (1989)
145454	No sign of duplicity in literature or SED fit
151044	Listed as a "probably suitable" calibrator in van Belle et al. (2008)
159139	No companion found using speckle in McAlister et al. (1987)
161693	No companion found using speckle in McAlister et al. (1987)
172569	Listed in "HIP Visual Binaries Kinematics" table by Bartkevicius & Gudas (2001); but no other information given in paper or general literature
182101	Used as calibrator in Berger et al. (2006)
184381	Used as comparison star in Johnson et al. (2006)
194012	Listed as a "suitable" calibrator in van Belle et al. (2008); no companion found using speckle in McAlister et al. (1987)
210074	Listed as a "suitable" calibrator in van Belle et al. (2008); used as comparison star in Wittenmyer et al. (2005)
217131	No companion found using speckle in McAlister et al. (1987)
219485	No sign of duplicity in literature or SED fit
222451	No sign of duplicity in literature or SED fit

Table 3. Exoplanet Host Stars' Calibrated Visibilities.

Target Name	MJD	B (m)	Θ (deg)	V_c	σV_c	% err
10697	53666.427	309.50	175.2	1.043	0.090	9
	53666.443	310.79	171.2	0.928	0.068	7
	53666.456	312.37	167.9	1.004	0.104	10
	53666.470	314.46	164.6	0.832	0.075	9
	54356.765	317.17	226.9	0.883	0.103	12
	54356.775	320.54	227.4	1.029	0.125	12
	54357.783	323.64	228.1	0.851	0.077	9
	54357.792	325.84	228.8	0.723	0.068	9
	54357.802	327.87	229.7	0.816	0.089	11
	54357.810	328.95	230.4	0.791	0.061	8
13189	53716.270	327.09	184.4	0.607	0.056	9
	53716.285	326.91	180.9	0.531	0.081	15
	53716.298	326.96	177.7	0.589	0.095	16
	53716.312	327.21	174.3	0.575	0.130	23
	53961.441	326.60	216.4	0.622	0.051	8
	53961.454	328.41	214.4	0.648	0.062	10
	53961.467	329.65	212.2	0.643	0.073	11
	53961.481	330.38	209.8	0.607	0.040	7
32518	54418.238	230.84	200.1	0.755	0.067	9
	54418.244	233.56	201.8	0.794	0.071	9
	54418.250	236.48	203.6	0.834	0.070	8
	54418.256	239.18	205.3	0.843	0.074	9
	54418.261	241.66	206.9	0.751	0.061	8
	54418.267	244.20	208.6	0.743	0.053	7
	54418.274	246.86	210.3	0.776	0.059	8
	54418.280	249.36	212.0	0.741	0.065	9
	54418.286	251.81	213.8	0.732	0.053	7
45410	54720.481	258.11	212.9	0.696	0.078	11
	54720.490	263.24	215.0	0.651	0.053	8
	54720.496	266.69	216.4	0.587	0.073	12
	54720.502	269.68	217.7	0.665	0.106	16
	54720.509	272.90	219.2	0.716	0.097	14
50554	53711.523	317.33	174.2	0.874	0.127	15
	53711.537	318.32	170.7	0.783	0.090	11
	53716.422	321.04	195.4	1.006	0.138	14
	53716.435	319.48	192.2	0.905	0.091	10
	53716.449	318.20	189.0	0.984	0.083	8
	53716.463	317.30	185.7	1.027	0.096	9
	53716.479	316.73	181.7	0.956	0.150	16
73108	54595.216	155.95	254.7	0.411	0.051	12
	54595.226	155.88	258.0	0.446	0.034	8
	54595.235	155.83	261.1	0.436	0.043	10
	54595.244	155.80	264.1	0.460	0.057	12
	54595.257	155.77	268.4	0.430	0.092	21

Table 3—Continued

Target Name	MJD	B (m)	Θ (deg)	V_c	σV_c	% err
136726	54595.294	147.57	189.4	0.442	0.055	12
	54595.307	148.79	193.7	0.425	0.045	11
	54595.315	149.53	196.5	0.468	0.054	12
	54595.325	150.30	199.6	0.421	0.056	13
	54595.336	151.17	203.4	0.436	0.062	14
	54595.346	151.80	206.5	0.409	0.053	13
139357	54357.149	320.57	102.8	0.450	0.070	16
	54357.155	320.14	104.2	0.460	0.045	10
	54357.161	319.66	105.6	0.487	0.063	13
	54357.167	319.12	107.1	0.491	0.066	13
	54358.151	320.24	103.9	0.460	0.030	7
	54358.157	319.77	105.3	0.415	0.034	8
	54358.162	319.27	106.7	0.429	0.049	11
145675	53958.259	329.81	168.4	0.902	0.054	6
	53958.275	329.38	164.9	0.878	0.045	5
	53958.292	328.62	161.0	0.859	0.051	6
	53959.168	329.99	189.3	1.096	0.123	11
	53959.184	330.18	185.5	1.000	0.089	9
	53959.200	330.26	181.8	0.964	0.069	7
	53959.215	330.26	178.1	0.990	0.070	7
	53959.231	330.18	174.5	0.940	0.078	8
	53959.246	330.01	170.9	0.954	0.067	7
	53959.261	329.70	167.4	0.808	0.064	8
154345	54719.168	328.79	90.5	0.885	0.094	11
	54719.179	328.73	93.3	0.843	0.109	13
	54719.185	328.66	94.7	0.811	0.089	11
	54719.192	328.57	96.2	0.803	0.096	12
	54719.198	328.45	97.6	0.847	0.096	11
	54719.204	328.29	99.2	0.903	0.095	11
	54719.213	328.00	101.4	0.817	0.122	15
164922	54689.201	326.49	248.8	0.663	0.089	13
	54689.212	325.27	251.2	0.820	0.058	7
	54689.223	324.07	253.6	0.957	0.079	8
	54689.235	322.84	256.4	1.067	0.153	14
	54689.248	321.74	259.4	1.011	0.170	17
167042	54358.232	321.20	97.5	0.584	0.037	6
	54358.238	320.96	99.0	0.551	0.036	7
	54358.243	320.68	100.3	0.507	0.036	7
	54358.249	320.34	101.7	0.524	0.030	6
	54358.255	319.96	103.1	0.571	0.036	6
	54358.261	319.53	104.5	0.612	0.037	6
	54358.267	319.05	105.9	0.591	0.041	7
	54358.273	318.48	107.4	0.627	0.050	8
170693	54346.303	187.40	183.8	0.373	0.042	11

Table 3—Continued

Target Name	MJD	B (m)	Θ (deg)	V_c	σV_c	% err
	54346.311	183.87	186.6	0.343	0.049	14
	54346.321	179.32	190.2	0.358	0.037	10
	54346.332	174.70	193.9	0.457	0.042	9
185269	54665.204	321.00	228.6	0.860	0.146	17
	54665.216	323.97	230.0	0.946	0.129	14
	54665.226	326.17	231.3	0.757	0.148	20
	54665.236	327.81	232.6	0.926	0.110	12
	54665.245	328.96	233.9	0.928	0.178	19
	54665.404	323.06	266.1	0.771	0.064	8
	54665.410	322.92	267.7	0.741	0.050	7
	54665.417	322.85	269.2	0.816	0.048	6
	54665.423	322.85	90.8	0.921	0.057	6
	54665.430	322.93	92.4	0.877	0.075	9
	54665.438	323.11	94.3	0.912	0.084	9
	54665.445	323.35	96.0	0.910	0.091	10
	54665.452	323.68	97.7	0.855	0.080	9
	54665.459	324.06	99.4	0.927	0.083	9
	54665.466	324.52	101.1	0.841	0.129	15
	54667.381	323.73	262.0	1.004	0.096	10
	54667.387	323.44	263.5	0.830	0.103	12
	54667.393	323.21	264.9	0.892	0.096	11
	54667.400	323.02	266.5	1.014	0.085	8
	54667.406	322.90	267.9	0.899	0.113	13
188310	54717.211	293.54	249.5	0.103	0.014	14
	54717.223	289.87	252.2	0.106	0.017	16
	54717.229	288.10	253.7	0.107	0.012	11
	54717.236	286.11	255.5	0.106	0.014	13
	54717.242	284.72	257.0	0.094	0.015	16
	54717.248	283.37	258.5	0.110	0.019	17
	54717.253	282.29	260.0	0.111	0.018	16
	54717.259	281.25	261.6	0.127	0.018	14
199665	54717.336	285.96	90.6	0.614	0.064	10
	54717.341	286.09	92.1	0.567	0.062	11
	54717.347	286.36	93.6	0.562	0.077	14
	54717.352	286.78	95.0	0.574	0.053	9
	54717.358	287.37	96.6	0.566	0.060	11
	54717.364	288.15	98.2	0.512	0.055	11
	54717.370	289.11	99.1	0.479	0.069	14
	54717.377	290.31	101.5	0.482	0.049	10
	54717.383	291.58	103.1	0.414	0.035	8
	54717.390	293.30	104.9	0.500	0.065	13
210702	54717.426	302.96	100.6	0.635	0.076	12
	54717.436	304.66	103.1	0.652	0.072	11
	54717.442	305.68	104.5	0.591	0.085	14

Table 3—Continued

Target Name	MJD	B (m)	Θ (deg)	V_c	σV_c	% err
	54717.448	306.87	105.9	0.640	0.091	14
217107	54717.283	292.41	236.3	0.771	0.096	12
	54717.289	289.09	237.2	0.793	0.127	16
	54717.296	285.35	238.3	0.757	0.095	13
	54717.303	281.40	239.5	0.799	0.118	15
	54717.309	278.11	240.6	0.776	0.114	15
221345	54720.234	313.74	229.1	0.278	0.031	11
	54720.239	315.41	229.9	0.253	0.034	13
	54720.245	317.13	230.8	0.266	0.028	11
	54720.250	318.64	231.7	0.232	0.024	10
	54720.256	320.12	232.7	0.251	0.028	11
222404	54664.457	253.07	230.4	0.105	0.011	10
	54664.466	254.63	233.0	0.099	0.011	11
	54664.475	256.07	235.6	0.091	0.010	11
	54720.278	247.87	222.5	0.104	0.012	12
	54720.285	249.26	224.5	0.093	0.010	11
	54720.295	251.32	227.6	0.093	0.008	9
	54720.301	252.45	229.3	0.086	0.008	9
	54720.307	253.58	231.2	0.092	0.009	10
	54720.313	254.70	233.2	0.091	0.008	9
	54720.320	255.83	235.2	0.087	0.009	10

Note. — The projected baseline position angle (Θ) is calculated to be east of north.

Table 4. Exoplanet Host Star and Planet Observed Parameters

	Observed Stellar Parameters					Planetary System Parameters			
HD	Spectral Type	$\theta_{\rm LD}$ (mas)	$\sigma_{\rm LD}$ %	K (mag)	π (mas)	$M_{\rm star}$ ($M_\odot$)	P (d)	Reference	(m-M)
10697	G5 IV	0.49 ± 0.05[a]	10	4.60 ± 0.02	30.70 ± 0.43	1.2	1076.4	Butler et al. (2006)	2.6
13189	K2	0.84 ± 0.03[a]	4	4.00 ± 0.03	1.78 ± 0.73	3.5[e]	472	P from Hatzes et al. (2005)	8.7
32518	K1 III	0.85 ± 0.02[b]	2	3.91 ± 0.04	8.29 ± 0.58	1.1	157.5	Döllinger et al. (2009b)	5.4
45410	K0 III-IV	0.97 ± 0.04[c]	4	3.70 ± 0.30	17.92 ± 0.47	1.7	889	Sato et al. (2008b)	3.7
50554	F8 V	0.34 ± 0.10[a]	29	5.47 ± 0.02	33.43 ± 0.59	1.1	1254	Fischer et al. (2002)	2.4
73108	K1 III	2.23 ± 0.02[b]	1	1.92 ± 0.07	12.74 ± 0.26	1.2	269.3	Döllinger et al. (2007)	4.5
136726	K4 III	2.34 ± 0.02[b]	1	1.92 ± 0.05	8.19 ± 0.19	1.8	516.2	Döllinger et al. (2009b)	5.4
139357	K4 III	1.07 ± 0.01[b]	1	3.41 ± 0.32	8.47 ± 0.30	1.3	1125.7	Döllinger et al. (2009a)	5.4
145675	K0 V	0.37 ± 0.04[a]	11	4.71 ± 0.02	56.91 ± 0.34	1.0	1724.0	Butler et al. (2003)	1.2
154345	G8 V	0.50 ± 0.03[c]	6	5.00 ± 0.02	53.80 ± 0.32	0.9	3360	Wright et al. (2008)	1.3
164922	K0 V	0.50 ± 0.07[d]	14	5.11 ± 0.02	45.21 ± 0.54	0.9	1155	Butler et al. (2006)	1.7
167042	K1 III	0.92 ± 0.02[b]	2	3.55 ± 0.24	19.91 ± 0.26	1.5	418	Sato et al. (2008b)	3.5
170693	K1.5 III	2.04 ± 0.04[b]	2	1.95 ± 0.05	10.36 ± 0.20	1.0	479.1	Döllinger et al. (2009a)	4.9
185269	G0 IV	0.48 ± 0.03[c]	6	5.26 ± 0.02	19.89 ± 0.56	1.3	6.8	Johnson et al. (2006)	3.5
188310	G9 III	1.73 ± 0.01[c]	1	2.17 ± 0.22	17.77 ± 0.29	2.2	137	Sato et al. (2008a)	3.8
199665	G6 III	1.11 ± 0.03[c]	3	3.37 ± 0.20	13.28 ± 0.31	2.2	993	Sato et al. (2008a)	4.4
210702	K1 III	0.88 ± 0.02[c]	2	3.98 ± 0.29	18.20 ± 0.39	1.9	341.1	Johnson et al. (2007)	3.7
217107	G8 IV	0.70 ± 0.01[c]	1	4.54 ± 0.02	50.36 ± 0.38	1.0	7.1	Fischer et al. (1999)	1.5
221345	G8 III	1.34 ± 0.01[c]	1	2.33 ± 0.24	12.63 ± 0.27	2.2	186	Sato et al. (2008b)	4.5
222404	K1 IV	3.30 ± 0.03[c]	1	1.04 ± 0.21	70.91 ± 0.40	1.6	906	Hatzes et al. (2003)	0.7

Note. — Spectral types are from *SIMBAD*; parallaxes π are from van Leeuwen (2007); K magnitudes are from Cutri et al. (2003), except for HD 73108, HD 136726, and HD 170693, which are from Neugebauer & Leighton (1969); (m-M) was calculated using Equation 3; [a]Baines et al. (2008a); [b]Baines et al. (2010); [c]Baines et al. (2009); [d]previously unpublished; [e]Mass from Schuler et al. (2005), though they cannot constrain the mass to better than 2-6$M_\odot$

Table 5. Calculated Parameters for Secondary Stars of Various Spectral Types

	G5 V			K0 V			K5 V			M0 V			M5 V		
HD	ΔK (mag)	α (mas)	θ (mas)	ΔK (mag)	α (mas)	θ (mas)	ΔK (mag)	α (mas)	θ (mas)	ΔK (mag)	α (mas)	θ (mas)	ΔK (mag)	α (mas)	θ (mas)
10697	1.5	80.6	0.26	1.9	78.8	0.24	2.5	77.2	0.21	3.1	74.9	0.17	4.1	70.1	0.08
13189	8.3	3.5	0.02	8.7	3.4	0.01	9.3	3.4	0.01	9.9	3.4	0.01	10.9	3.3	0.00
32518	5.0	6.0	0.07	5.4	5.9	0.07	6.0	5.8	0.06	6.6	5.6	0.05	7.6	5.2	0.02
45410	3.5	44.7	0.15	3.9	43.9	0.14	4.5	43.2	0.12	5.2	42.2	0.10	6.2	40.2	0.05
50554	0.4	95.6	0.29	0.8	93.5	0.26	1.4	91.4	0.22	2.1	88.5	0.19	3.0	82.5	0.08
73108	6.1	13.4	0.11	6.5	13.1	0.10	7.1	12.9	0.09	7.7	12.5	0.07	8.7	11.7	0.03
136726	7.0	14.4	0.07	7.4	14.2	0.06	8.0	13.9	0.05	8.7	13.6	0.05	9.6	13.0	0.02
139357	5.5	23.4	0.07	5.9	23.0	0.07	6.5	22.5	0.06	7.1	21.9	0.05	8.1	20.6	0.02
145675	0.0	199.0	0.49	0.4	194.4	0.45	1.0	190.0	0.38	1.7	183.7	0.32	2.6	170.6	0.14
154345	-0.2	287.3	0.46	0.2	280.3	0.43	0.8	273.4	0.36	1.5	263.6	0.30	2.5	243.1	0.14
164922	0.1	119.8	0.39	0.5	116.9	0.36	1.1	114.2	0.30	1.8	110.2	0.25	2.7	102.0	0.11
167042	3.5	29.2	0.17	3.9	28.7	0.16	4.5	28.2	0.13	5.1	27.5	0.11	6.1	26.0	0.05
170693	6.5	15.4	0.09	6.9	15.0	0.08	7.5	14.7	0.07	8.1	14.2	0.06	9.1	13.2	0.03
185269	1.7	1.8	0.17	2.1	1.8	0.16	2.7	1.7	0.13	3.4	1.7	0.11	4.4	1.6	0.05
188310	5.1	13.5	0.15	5.5	13.3	0.14	6.1	13.1	0.12	6.7	12.9	0.10	7.7	12.4	0.04
199665	4.5	37.8	0.11	4.9	37.3	0.11	5.5	36.8	0.09	6.2	36.1	0.07	7.1	34.7	0.03
210702	3.2	24.4	0.16	3.6	24.0	0.14	4.2	23.7	0.12	4.9	23.2	0.10	5.8	22.1	0.05
217107	0.5	4.5	0.43	0.9	4.4	0.40	1.5	4.3	0.34	2.1	4.1	0.28	3.1	3.8	0.13
221345	5.7	11.8	0.11	6.1	11.6	0.10	6.7	11.4	0.08	7.3	11.2	0.07	8.3	10.8	0.03
222404	3.2	176.6	0.61	3.6	173.5	0.56	4.2	170.5	0.48	4.9	166.4	0.40	5.8	158.1	0.18

Note. — Values for M_K (used to calculate ΔK), secondary stellar masses (used to calculate α), and secondary stellar radii (used to calculate θ) were obtained from Cox (2000): G5 V = 3.5, 0.92 $M_\odot$, 0.92 $R_\odot$; K0 V = 3.9, 0.79 $M_\odot$, 0.85 $R_\odot$; K5 V = 4.5, 0.67 $M_\odot$, 0.72 $R_\odot$; M0 V = 5.2, 0.51 $M_\odot$, 0.60 $R_\odot$; M5 V = 6.1, 0.21 $M_\odot$, 0.27 $R_\odot$.

Table 6. Observed Diameter Fit Residuals and Calculated Binary Visibility Residuals

			$\Delta V_{\max}$, PA=0°					$\Delta V_{\max}$, PA=30°					$\Delta V_{\max}$, PA=60°				
HD	Obs Date	$\sigma_{\rm res}$	G5V	K0V	K5V	M0V	M5V	G5V	K0V	K5V	M0V	M5V	G5V	K0V	K5V	M0V	M5V
10697	2005 Oct 23	0.092	0.221	0.162	0.098	0.058	0.024	0.232	0.164	0.096	0.055	0.022	0.225	0.162	0.098	0.058	0.024
	2007 Sep 14	0.053	0.221	0.162	0.098	0.058	0.024	0.232	0.164	0.096	0.055	0.022	0.225	0.162	0.098	0.058	0.024
13189	2005 Dec 12	0.033	0.001	0.000	0.000	0.000	0.000	0.001	0.000	0.000	0.000	0.000	0.001	0.000	0.000	0.000	0.000
	2006 Aug 14	0.019	0.001	0.000	0.000	0.000	0.000	0.001	0.000	0.000	0.000	0.000	0.001	0.000	0.000	0.000	0.000
32518	2007 Nov 14	0.036	0.011	0.008	0.005	0.003	0.001	0.012	0.008	0.005	0.003	0.001	0.011	0.008	0.005	0.003	0.001
45410	2008 Sep 11	0.052	0.047	0.033	0.019	0.010	0.004	0.046	0.032	0.019	0.010	0.004	0.047	0.033	0.019	0.010	0.004
50554	2005 Dec 12	0.047	0.448	0.346	0.213	0.112	0.057	0.445	0.365	0.238	0.135	0.062	0.485	0.384	0.244	0.137	0.061
73108	2008 May 09	0.018	0.200	0.201	0.202	0.202	0.202	0.201	0.201	0.201	0.202	0.202	0.199	0.201	0.202	0.202	0.202
136726	2008 May 09	0.018	0.194	0.194	0.194	0.194	0.195	0.194	0.194	0.194	0.194	0.195	0.193	0.194	0.194	0.194	0.195
139357	2007 Sep 14	0.019	0.008	0.005	0.003	0.002	0.001	0.008	0.005	0.003	0.002	0.001	0.008	0.005	0.003	0.002	0.001
145675	2006 Aug 12	0.056	0.543	0.460	0.302	0.166	0.076	0.401	0.420	0.301	0.165	0.046	0.542	0.459	0.302	0.169	0.077
154345	2008 Sep 10	0.039	0.256	0.336	0.282	0.186	0.094	0.493	0.529	0.391	0.233	0.099	0.272	0.361	0.328	0.211	0.094
164922	2008 Aug 11	0.161	0.564	0.489	0.322	0.183	0.082	0.608	0.481	0.306	0.167	0.069	0.562	0.487	0.321	0.183	0.082
167042	2007 Sep 15	0.040	0.045	0.032	0.019	0.011	0.004	0.046	0.032	0.019	0.011	0.004	0.046	0.032	0.018	0.011	0.004
170693	2007 Sep 03	0.037	0.219	0.219	0.220	0.220	0.220	0.219	0.219	0.220	0.220	0.220	0.218	0.219	0.220	0.220	0.220
185269	2008 Jul 18	0.078	0.193	0.139	0.086	0.047	0.019	0.203	0.146	0.087	0.047	0.018	0.137	0.098	0.058	0.032	0.013
	2008 Jul 20	0.079	0.193	0.139	0.086	0.047	0.019	0.203	0.146	0.087	0.047	0.018	0.137	0.098	0.058	0.032	0.013
188310	2008 Sep 08	0.012	0.151	0.152	0.153	0.154	0.155	0.151	0.152	0.153	0.154	0.155	0.152	0.152	0.153	0.154	0.155
199665	2008 Sep 08	0.054	0.020	0.014	0.008	0.004	0.002	0.020	0.014	0.008	0.004	0.002	0.020	0.014	0.008	0.004	0.002
210702	2008 Sep 08	0.025	0.060	0.042	0.024	0.013	0.006	0.059	0.041	0.024	0.013	0.006	0.059	0.041	0.024	0.013	0.006
217107	2008 Sep 08	0.017	0.496	0.376	0.239	0.148	0.061	0.499	0.374	0.234	0.140	0.059	0.454	0.339	0.213	0.131	0.058
221345	2008 Sep 11	0.013	0.007	0.005	0.003	0.002	0.001	0.007	0.005	0.003	0.002	0.001	0.007	0.005	0.003	0.002	0.001
222404	2008 Sep 11	0.006	0.182	0.187	0.192	0.196	0.198	0.182	0.187	0.192	0.196	0.198	0.182	0.187	0.192	0.196	0.198

Note. — PA is the position angle.

Table 7. Eliminating Certain Secondary Stars

		PA=0°					PA=30°					PA=60°				
HD	Obs Date	G5V	K0V	K5V	M0V	M5V	G5V	K0V	K5V	M0V	M5V	G5V	K0V	K5V	M0V	M5V
10697	2005 Oct 23	X	P	P	P	P	X	P	P	P	P	X	P	P	P	P
	2007 Sep 14	X	X	P	P	P	X	X	P	P	P	X	X	P	P	P
13189	2005 Dec 12	P	P	P	P	P	P	P	P	P	P	P	P	P	P	P
	2006 Aug 14	P	P	P	P	P	P	P	P	P	P	P	P	P	P	P
32518	2007 Nov 14	P	P	P	P	P	P	P	P	P	P	P	P	P	P	P
45410	2008 Sep 11	P	P	P	P	P	P	P	P	P	P	P	P	P	P	P
50554	2005 Dec 12	X	X	X	X	P	X	X	X	X	P	X	X	X	X	P
73108	2008 May 09	X	X	X	X	X	X	X	X	X	X	X	X	X	X	X
136726	2008 May 09	X	X	X	X	X	X	X	X	X	X	X	X	X	X	X
139357	2007 Sep 14	P	P	P	P	P	P	P	P	P	P	P	P	P	P	P
145675	2006 Aug 12	X	X	X	X	P	X	X	X	X	P	X	X	X	X	P
154345	2008 Sep 10	X	X	X	X	X	X	X	X	X	X	X	X	X	X	X
164922	2008 Aug 11	X	X	P	P	P	X	X	P	P	P	X	X	P	P	P
167042	2007 Sep 15	P	P	P	P	P	P	P	P	P	P	P	P	P	P	P
170693	2007 Sep 03	X	X	X	X	X	X	X	X	X	X	X	X	X	X	X
185269	2008 Jul 18	X	P	P	P	P	X	P	P	P	P	P	P	P	P	P
	2008 Jul 20	X	P	P	P	P	X	P	P	P	P	P	P	P	P	P
188310	2008 Sep 08	X	X	X	X	X	X	X	X	X	X	X	X	X	X	X
199665	2008 Sep 08	P	P	P	P	P	P	P	P	P	P	P	P	P	P	P
210702	2008 Sep 08	X	P	P	P	P	X	P	P	P	P	X	P	P	P	P
217107	2008 Sep 08	X	X	X	X	X	X	X	X	X	X	X	X	X	X	X
221345	2008 Sep 11	P	P	P	P	P	P	P	P	P	P	P	P	P	P	P
222404	2008 Sep 11	X	X	X	X	X	X	X	X	X	X	X	X	X	X	X

Note. — "X" indicates a secondary star of that spectral type can be ruled out from the observations, while "P" means a secondary star with that spectral type is still a possibility in the system.

Table 8. Angular Diameter Comparison

HD	$\theta_{\rm LD}$ (mas)	$\theta_{\rm SED}$ (mas)	$\theta_{(V-K)}$ (mas)
10697	0.49 ± 0.05	0.50 ± 0.03	0.53 ± 0.02
13189	0.84 ± 0.03	0.80 ± 0.04	0.97 ± 0.04
32518	0.85 ± 0.02	0.89 ± 0.10	0.84 ± 0.04
45410	0.97 ± 0.04	0.87 ± 0.07	0.87 ± 0.37
50554	0.34 ± 0.10	0.33 ± 0.01	0.34 ± 0.01
73108	2.23 ± 0.02	2.12 ± 0.15	2.44 ± 0.75
136726	2.34 ± 0.02	2.46 ± 0.34	2.30 ± 0.88
139357	1.07 ± 0.01	1.40 ± 0.28	1.07 ± 0.49
145675	0.37 ± 0.04	0.51 ± 0.01	0.53 ± 0.01
154345	0.50 ± 0.03	0.43 ± 0.02	0.45 ± 0.01
164922	0.50 ± 0.07	0.39 ± 0.02	0.44 ± 0.02
167042	0.92 ± 0.02	0.88 ± 0.07	0.98 ± 0.33
170693	2.04 ± 0.04	1.90 ± 0.16	2.03 ± 0.62
185269	0.48 ± 0.03	0.34 ± 0.02	0.38 ± 0.01
188310	1.73 ± 0.01	1.68 ± 0.06	1.88 ± 0.59
199665	1.11 ± 0.03	0.99 ± 0.03	1.01 ± 0.29
210702	0.88 ± 0.02	0.83 ± 0.07	0.74 ± 0.31
217107	0.70 ± 0.01	0.52 ± 0.02	0.54 ± 0.02
221345	1.34 ± 0.01	1.43 ± 0.14	1.86 ± 0.63
222404	3.30 ± 0.03	3.06 ± 0.16	2.98 ± 0.87

Note. — For the SED and $(V-K)$ fits, the photometric values used are from the following sources: UBV from Mermilliod (1991) for all stars except HD 13189 and HD 50554 (BV only from ESA 1997); RI from Monet et al. (2003); and JHK from Cutri et al. (2003). $T_{\rm eff}$ and log g values were from Allende Prieto & Lambert (1999) for all stars except HD 13189 and HD 50554 (Soubiran et al. 2010); HD 136726 (Cayrel de Strobel et al. 1997); HD 154345 (Prugniel et al. 2007); and HD 32518 and HD 139357, which are from Cox (2000) and were based on their spectral types as listed in the *SIMBAD Astronomical Database*.

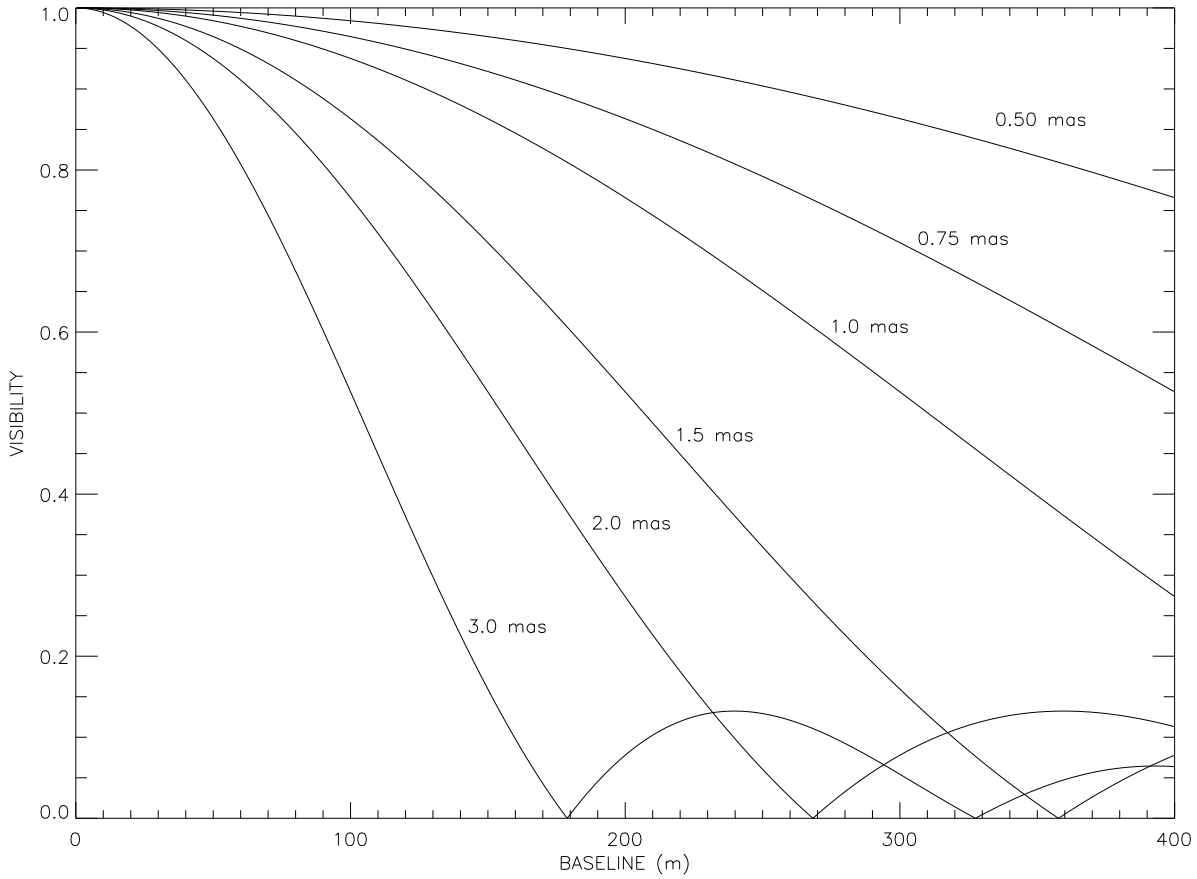

Fig. 1.— The effect of various stellar angular diameters on the visibility curve. The smaller a star's angular diameter, the less change is seen in the visibility curve as a function of baseline.

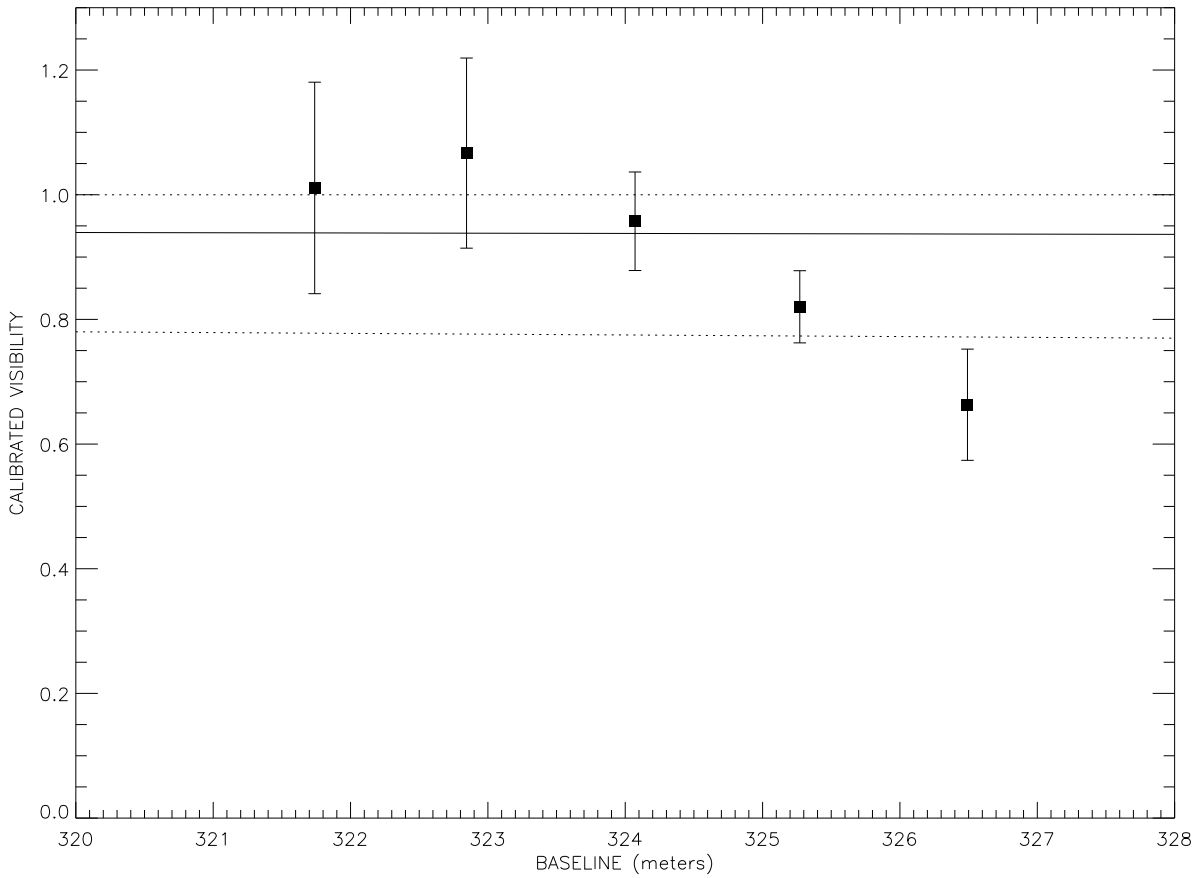

Fig. 2.— HD 164922 LD disk diameter fit. The solid line represents the theoretical visibility curve for the star with the best fit $\theta_{\rm LD}$, the dashed lines are the 1σ error limits of the diameter fit, the squares are the calibrated visibilities, and the vertical lines are the measured errors.

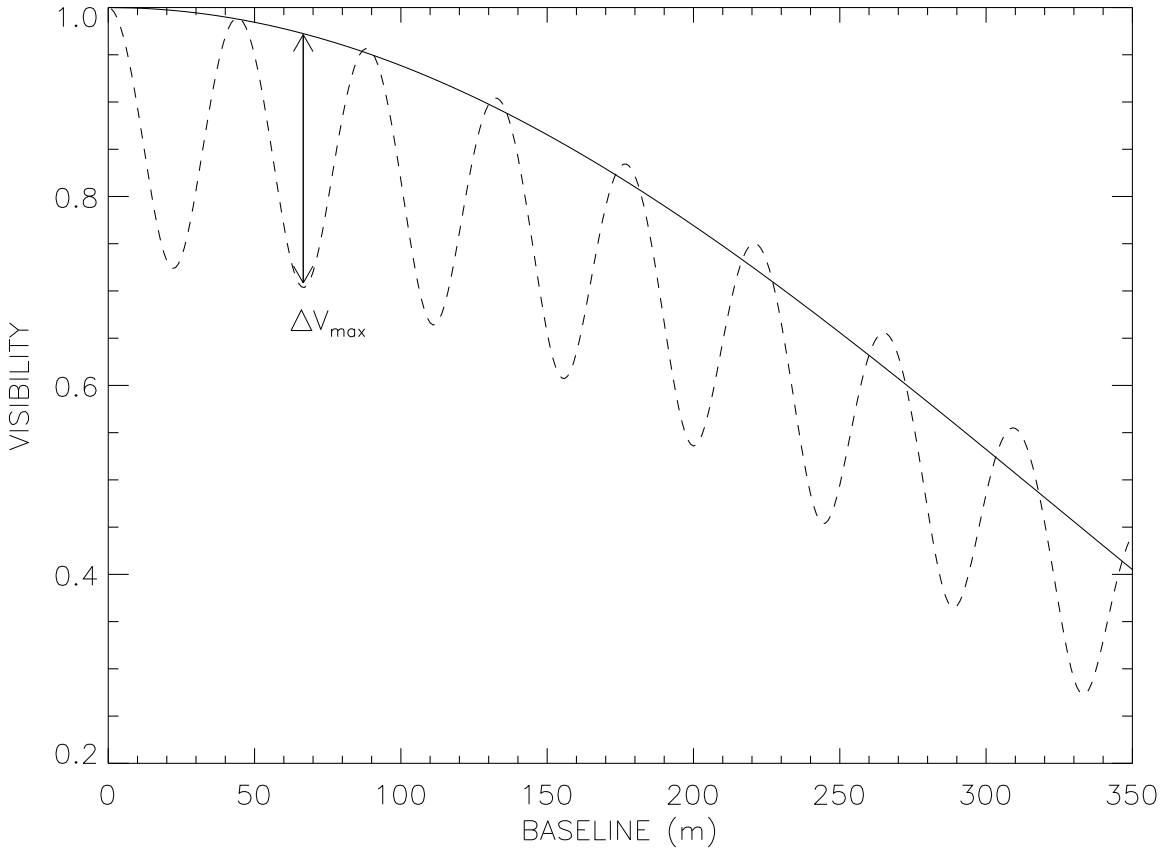

Fig. 3.— Example of the difference between the visibility curves for a single star and a binary system. The solid line indicates the curve for a single star with θ=1.0 mas, while the dashed line represents the curve for a binary system with the following parameters: $\theta_{\rm primary}$=1.0 mas, $\theta_{\rm secondary}$=0.5 mas, α=10 mas, and ΔK=2.0. $\Delta V_{\rm max}$ is the maximum deviation between the two curves.

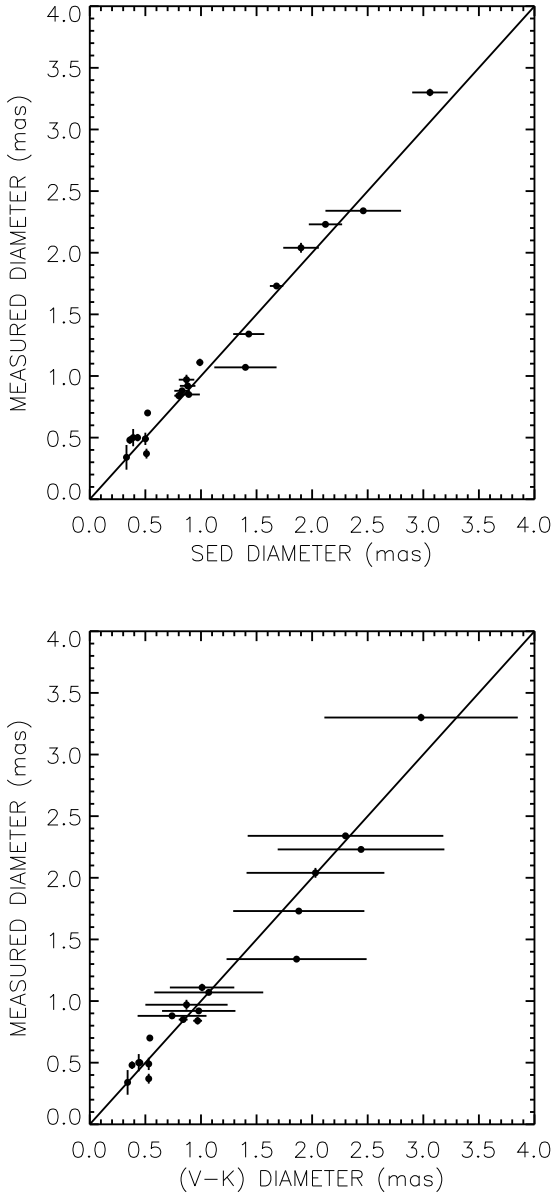

Fig. 4.— A comparison of estimated and interferometrically-measured angular diameters. The upper and lower panels compare diameters derived using SED fits and $(V-K)$ colors, respectively, versus diameters measured using the CHARA Array. Note the larger error bars associated with the SED and $(V-K)$ diameters for stars larger than $\sim$0.7 mas.